DESIGN AND NUMERICAL INVESTIGATION ON A PASSIVE MICRO T-MIXER WITH TAIL-ADDED OBSTACLES

Phu Nguyen Van[1], Van-Anh Bui[1], Thanh Pham Van[1], Quynh Luu Manh[2], Nam Nguyen Hoang[3], Tien Nguyen Chung[4], Van Nguyen Thi Thanh[4*]

[1] Faculty of Physics, VNU University of Science, Vietnam National University, Hanoi

[2]Center for Material of Science, VNU University of Science, Vietnam National University, Hanoi

[3]Nano and Energy Center, VNU University of Science, Vietnam National University, Hanoi

[4]Vietnam Academy of Cryptography Techniques

*Email: nguyenthithanhvancms@gmail.com

Received: 16/11/2022; Received in revised form: 17/11/2022; Accepted: 4/8/2023

ABSTRACT

In this paper, the type of obstacle micromixer model was designed and investigated by numerical simulation to improve the mixing efficiency. Passive mixers with tail-added obstacles structures were studied and compared with other conventional T microstructures, and then their mixing performance was numerically evaluated. The micro-T mixer with tail-added obstacles (μTTAO) exhibited a higher mixing efficiency and reached 87.2%. In addition, the concentration range at the outlet was also narrow, the mixing efficiency was increased by about 1.41 compared with the normal micro-T mixer. The combination of grooves greatly enhances the mixing in the flow path due to strong turbulence. The combination of multiple tracks in the fluidic structure enhances the micromixer's performance by reducing mixing time. In addition, the influence of the length and number of obstacles in the microchannel has also been studied extensively. This study shows that increasing the number or length of obstacles in the microchannel optimally improves the mixing efficiency value. The results further demonstrated that going beyond the performance of the micro-T mixer with obstacles, the μTTAO is a potential structure for optimizing the mixing quality of the micro-T mixer. This study is a significant turning point with high efficiency and low cost in the future.

Keywords: Grooves; Mixing simulation; Passive mixer; T-shaped channel.

1. INTRODUCTION

In the past decade, various instruments in the field of microfluidics have been developed for the analysis of biological and chemical targets in the research areas of biomedical diagnostics, food safety control, and environmental protection. Microfluidic use in various applications has received increasing attention due to its compact size, automatic operation, faster detection, fewer reagents, higher sensitivity, and integration capability [1]–[6]. Studies typically integrate injection, mixing, reacting, washing, separation, and detection onto a centimeter-level chip [7]. In the research field of biological, chemical, or medical reaction processes, many reagents must be mixed before a reaction can occur. The mixing process must be rapid and even so that the reaction can develop fully, and the reaction dynamics can be studied. Among them, micromixers are one of the most important components of micro-scale fluid devices, which significantly affect the performance and sensitivity of fluid systems.

Micromixer is one of the most important components of a microfluidic device where the mixing of fluids becomes critical, like in reagents such as small molecules, large macromolecules, and particles. At the micro-scale, the mixing process often depends on convection effects and achieves heat and mass transfer efficiency. Due to the small dimensions and high surface–to–volume ratio, the micro-scale fluidic devices present unique and very different physical mechanisms compared to the macroscopic ones. In addition, the mixing efficiency is also significantly dependent on the molecular diffusion mechanism, which is a slow process and may require microchannel stretching to achieve the desired mixing quality [8]. Therefore, the mixing efficiency can be considered a key parameter for a micromixer and one of the most fundamental challenges.

Based on the principles used to perform the mixing process at the microscale, micromixers are generally classified into two types: passive micromixers and active micromixers. Active micromixers use actuators to improve mixing efficiency by stirring liquid flow using external forms of energy supply such as electrokinetic time pulsed [5]–[7], [9], magnetic field and heat, and pressure perturbation [10]. Active mixer construction usually requires an external power source, such as an electric field, magnetic field, and sound. In contrast, passive micromixers require no external power input except the power to drive fluids and commonly used complex channel geometries to enhance turbulent diffusion or convection. The active micromixers' structure is usually relatively simple and easier to control, but the requirements of external energy sources make it harder for them to assimilate. Passive mixers are much easier integrated into microfluidic devices, but they often require complex fabrication processes to create the desired structure. The passive micromixer relies on its geometry to enhance the mixing efficiency and has strong system stability, so it was widely used in microfluidic

systems. Among them, the T-shaped passive micromixers structure is more straightforward to manufacture than other passive micromixers because of its simple geometry.

In this study, the micromixer with tail-added obstacles model is designed and investigated by numerical simulation to improve mixing efficiency. The design of the proposed mixing structure utilizes twisted microchip systems to increase the fluid transfer inside the fluidic channel. The tail-added obstacles were intentionally added along the microchannel to increase turbulent advancement and facilitate the mixing process. Passive mixers with tail-added obstacles structures were studied and compared with other conventional T microstructures. In addition, the tail length and the number of tail-added obstacles which increase the mixing channel performance were also studied, simulated, and calculated.

2. MIXING STRUCTURE

The basic design of a micro-T mixer is a passive micromixer with two inputs and one output, as shown in Fig. 1 (a). The main channel was designed with a length of 800 μm and a width of 100 μm. The width of the inlet microchannels was equal to 50 μm. The micro-T mixer was added with 11 obstacles in the main channel, as shown in Fig. 1 (b), to improve the mixing efficiency compared to the normal channel. The obstacles were tilted at an angle of 45 degrees to the vertical and designed to be $50\sqrt{2}$ μm in length.

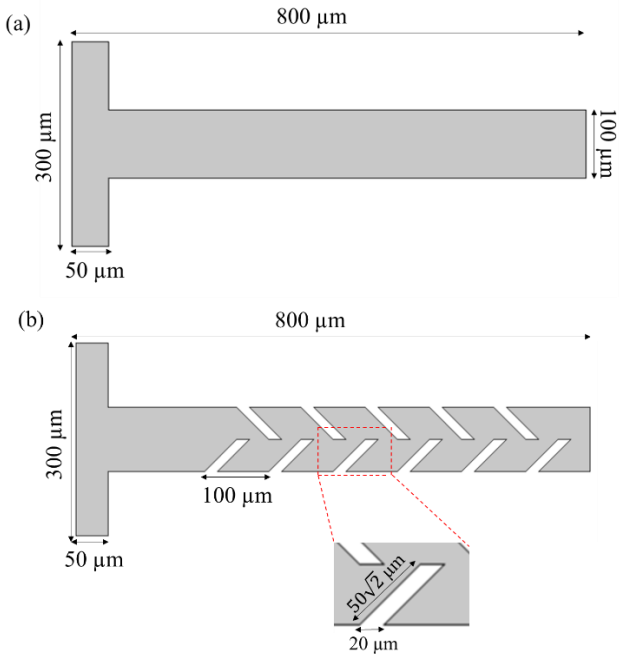

Fig. 1. Mixing Geometry of two fluids in a micro-T mixer (a) without and (b) with obstacles

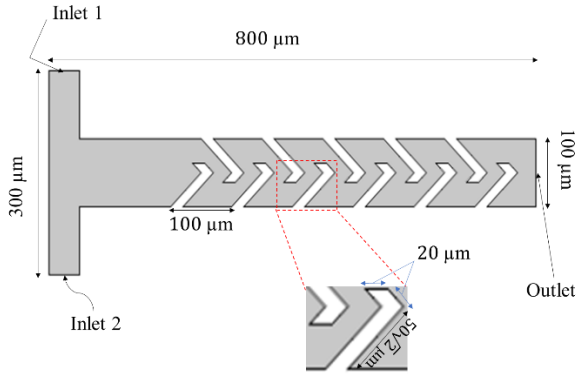

Fig. 2. Mixing Geometry of two fluids in a µTTAO

In this study, we propose a micro-T mixer with tail–added obstacles (µTTAO), which was designed similarly to the conventional micro-T mixer with obstacles and added tails. Each tail was designed with a length of 20 µm, as shown in Fig. 2.

3. SIMULATION

3.1 Model Parameters and Physics

In this work, the numerical simulation was performed in COMSOL Multiphysics 5.6 software. The mass transport and fluid flow equations are simulated with suitable boundary conditions. The finite element method was used to solve those equations.

The T-mixer model was designed with two inputs fed by different concentrations of 1 M and 0 M, respectively. Blood and water, two low-diffusivity liquids, were used and analyzed in the simulation. The properties of the fluids are shown in Table 1.

Table 1. Fluid and physical properties are used in the simulation model [11].

Properties	Value	Unit
Blood density	1060	kg/m^3
Blood viscosity	4	$mPa{\cdot}s$
Water density	1000	kg/m^3
Water viscosity	1	$mPa{\cdot}s$
Diffusivity	7.55×10^{-11}	m^2/s
Velocity	3×10^{-4}	m/s

The diffusivity of blood and water, D is calculated using the Stokes-Einstein Equation [12]:

$$D = \frac{KT}{6\pi\eta R_1} m^2/s \quad (1)$$

Where K is the Boltzmann constant ($1.38 \times 10^{-23} J/K$), T is the temperature (K), R_1 is the radius of the molecule of solute (m), η is the viscosity of the solvent ($Pa.s$). The diffusivity, D, is calculated as $7.55 \times 10^{-11}\ m^2/s$.

The inlet of the channel was fed a liquid flow with a velocity of 3×10^{-4} m/s while the outlet of the channel was set at a pressure of 0 Pa. At the microchannel wall, the boundary condition was no slip for fluid velocity and impermeability of ions. The corresponding equations are:

$$u = 0 \quad (2)$$

$$n.J_i = 0 \quad (3)$$

Where u is the velocity (m/s), J is the flux density of species i.

The other physical properties used in the simulation are shown in Table I. A set of physical interfaces in the microfluidic channel was designed to examine the simulation model. In 2D modeling, physical models such as laminar flow and transport of diluted species were applied.

3.2 Governing Equation

In this study, the velocity and pressure of liquid flow in the channel were simulated with laminar channel conditions. Specifically, in this case, the Navier - Stokes equation is solved for an uncompressed stream in the time domain [13]:

$$\rho\left(\frac{\partial u}{\partial t} + u.\nabla u\right) = -\nabla p + \nabla.\mu\nabla u \quad (4)$$

$$\nabla.u = 0 \quad (5)$$

Where u is the local velocity (m/s), ρ is the pressure (Pa), μ is the liquid viscosity ($Pa.s$), and $-\nabla p$ is the pressure gradient.

For co-laminar flow, diffusion is dominant in mixing and is defined as the process by which a molecule propagates in a channel from an area of higher concentration to an area of lower concentration. The description of diffusion is governed by Fick's Law [14]:

$$N_i = -D_i\nabla c_i \quad (6)$$

$$\frac{\partial c_i}{\partial t} = D_i\nabla^2 c_i \quad (7)$$

Where N_i, D_i and c_i is the molar flux ($\mathrm{mol.m^{-2}.s^{-1}}$), diffusion coefficient ($\mathrm{m^2.s^{-1}}$) and the concentration ($\mathrm{mol.m^{-3}}$), respectively.

3.3. Performance Evaluation Parameters

The simulation results allow us to obtain detailed calculation results of the concentration of the liquid at each different point. Therefore, to evaluate the mixing quality of each different geometry, we averaged the concentration values at different points along the slice at the outlet, corresponding to the equation:

$$MI = 1 - \sqrt{\frac{1}{N}\sum_{j=1}^{N}\left(\frac{c_j - \bar{c}}{\bar{c}}\right)^2} \quad (8)$$

Where MI is the mixing index, N is the total number of points to sample, c_j is the concentration of the liquid at point j (*mol*), and $\bar{c}$ is the average concentration of the liquid at the outlet (*mol*).

With the calculation MI = 0, i.e., no mixing occurs, while MI = 1 means the mixing result is perfect. However, it is challenging for the mixing index to reach 100% in practice. Therefore, the mixing quality is considered perfect when the mixing index is greater than 0.8 [15].

4. RESULTS AND DISCUSSING

4.1 Velocity distribution

For all three different geometries, the fluidic channel structure greatly influenced the flow field in the channel. In this study, the flow colliding with obstacles in the channel dramatically changed the velocity field. Fig. 4 shows the velocity distribution in the different micro-T mixer structures. The results show that the fluid particles moved parallel in the channel wall for a regular micro-T mixer and reached the maximum value at the center channel, as shown in Fig. 4 (a).

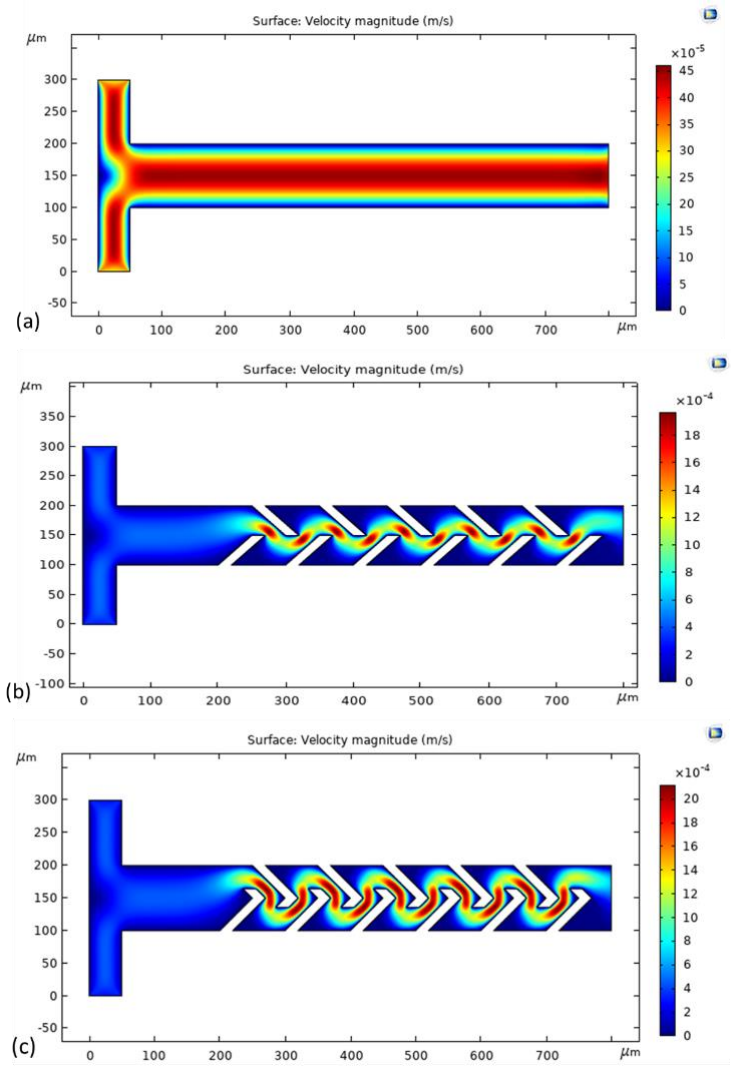

Fig.4. Velocity distribution of micro-T mixer (a) without, (b) with obstacles, and (c) with tail–added obstacles.

For the other two structures, the obstacles created vortices around them. Therefore, the velocity flow will be blocked and change direction. It is predicted that the additional effect of adding tails to the obstacles will cause the horizontal velocity component to change more. This made the fluid flow in the channel facilitate mixing and achieved better mixing quality. The velocity field results depicted in Fig. 4 (b) – (c) show that the micro-T mixer added tail obstacles create a giant vortex around and significantly change the horizontal velocity. These acquired results also indicate that the mixing quality of the passive microfluidic mixing channel depends mainly on the channel geometry.

4.2 The comparison between passive micro-T mixers

The normal micro-T mixer had no obstacle in the channel, and the fluid flow in the channel was laminar. Therefore, the diffusion of two liquids inside the channel was the only mixing mechanism. At the outlet of the normal micro-T mixer, the mixing of the two liquids was not uniform, as shown in Fig. 5 (a).

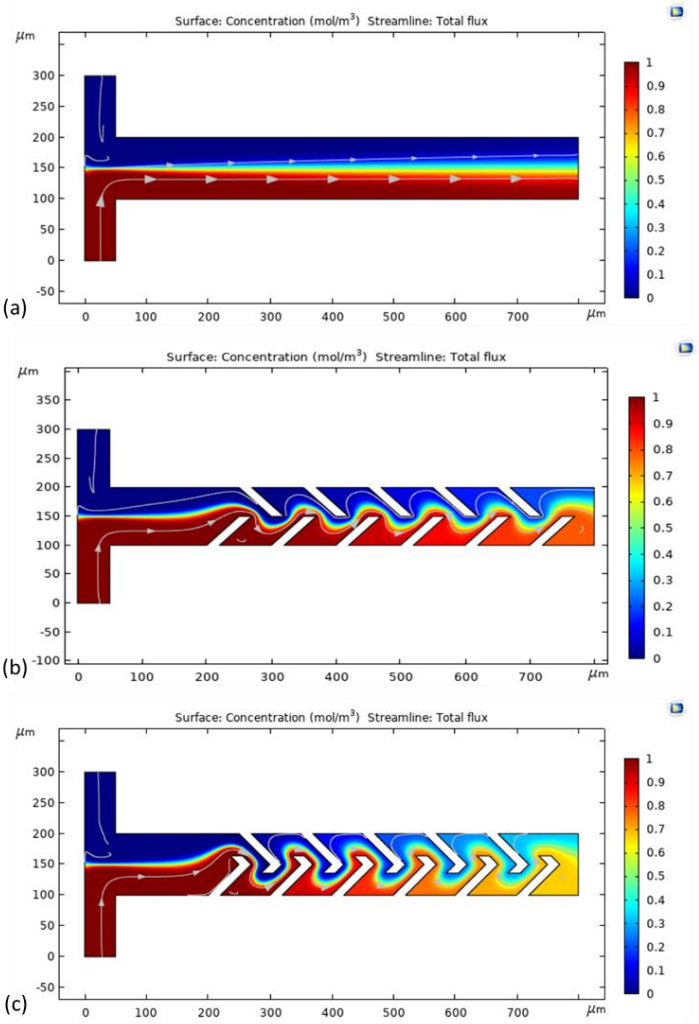

Fig.4. Concentration profiles of micro-T mixer (a) without, (b) with obstacles, and (c) with tail–added obstacles.

Regarding the micro-T mixer with obstacles (TMWO), as discussed in the previous section, the fluid was mixed uniformly at the outlet of the channel, as shown in fig. 5 (b). This improvement is due to the convective effects associated with the transversal flows generated by the asymmetric obstacles. Fig. 5 (c) shows the distribution of fluidic concentration in the channel of the μTTAO structure. In this construction, obstacles have been added with the tails, which causes the contact surface to be enlarged and enhances mixing efficiency.

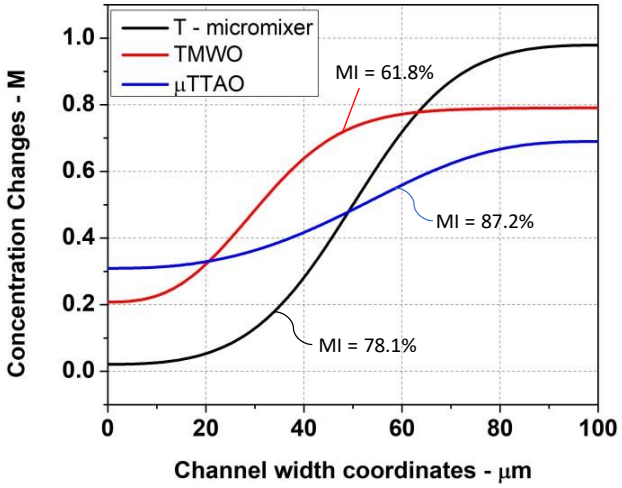

Fig.5. Concentration and mixing index of the values at the outlet

Figure 5 shows the concentration and mixing index at the outlet of three different mixing geometries. For a normal micro-T mixer, the concentration value at the outlet was changed from 0 to 1 M, and the mixing index reached 61.8%. For a micro-T mixer with obstacles, by adding obstacles, the mixing efficiency was increased significantly to about 78.1%. At the same time, the concentration range at the outlet was also narrower, and thus mixing quality was increased by 1.26 times compared with a normal micro-T mixer. For a micro-T mixer with tail-added obstacles, the mixing index was 87.2%, which exhibits 1.41 times higher than a normal micro-T mixer. The results further demonstrated that going beyond the performance of the micro-T mixer with obstacles, the µTTAO is a potential structure for optimizing the mixing quality of the micro-T mixer.

4.3 Impact of the length of the tail on mixing efficiency

In this work, the impact of tail length, ranging from 20 µm to 45 µm, on the channel's mixing quality was investigated. With an increase in the length of the tails, the direction of fluid movement hung more strongly, enhancing the turbulent convection in the microchannel. The rise in the tail length causes a greater change in the horizontal velocity component, resulting in the mixing efficiency enhancement. Figure 7 shows the significant dependence of the mixing index at the outlet on the tail length. Regarding the tail length of 45 µm, the mixing quality was achieved at 95.3%, while the figure was only 87.2% with a tail length of 20 µm. It can be concluded that the tail length increases, and so does the mixing index.

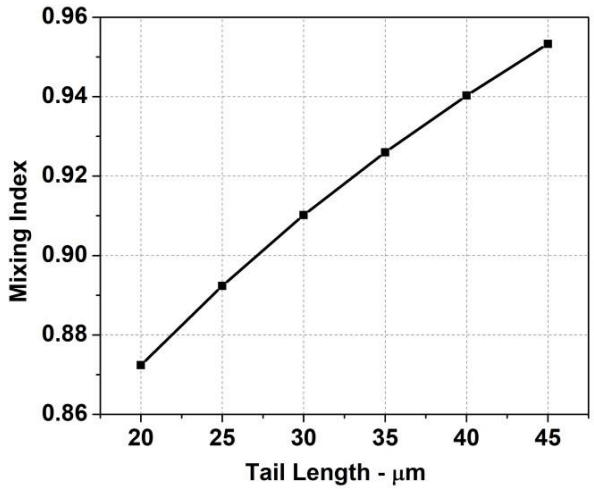

Fig.7. The dependence of the mixing index at the outlet on the tail length.

4.4 Impact of the number of tail-added obstacles on mixing efficiency

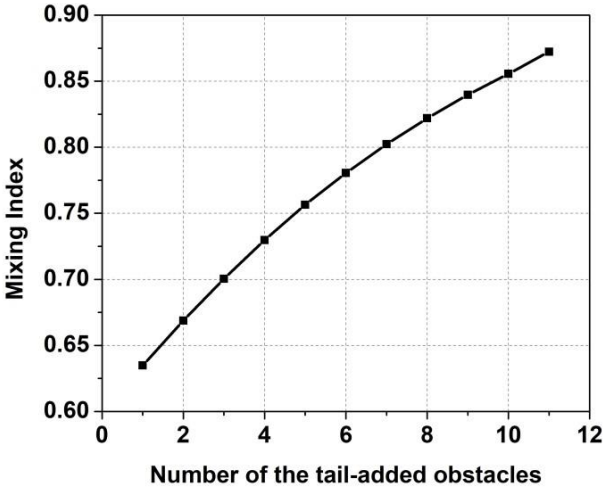

Fig.8. The dependence of the mixing index at the outlet on the number of tail-added obstacles.

In addition, the influence of the number of the tail–added obstacles on the mixing index was also evaluated in this study. Figure 8 demonstrates the significant dependence of the mixing index at the outlet on the number of tail-added obstacles. Regarding the channel with only a tail-added obstacle, the mixing index reached only 63.5%. In contrast, for a channel with a tail-added obstacles count of 11, the mixing index increased 1.37 times and reached 87.2%. At this point, the mixing efficiency took place in the near-perfect channel. This result can be explained because when the number of the tail-added obstacles was increased, the vortex created by the tail-added obstacles in the channel was also increased, causing the fluid flow through the channel to be bumped and blocked at more locations, which resulted in improved mixing quality. Therefore, increasing the number of tail-added obstacles is one of the straightforward methods to optimize the mixing efficiency of the mixing channel.

5. CONCLUSION

In this study, a micro-T mixer structure with tail-added was proposed and numerically evaluated to improve the mixing efficiency of the conventional micromixer. The obstacles created a turbulent mixing inside the channel by causing flow consolidation. Despite the complexity of the proposed structure, going beyond the performance of the micro-T mixer with obstacles, the proposed μTTAO rose the mixing efficiency by 1.41 times compared to conventional T-shaped mixers without obstacles. The dependences of the mixing performance on the size of the tail-added obstacles and the number of obstacles were also studied and evaluated. This research work verifies the effectiveness and feasibility of the proposed μTTAO structure in biological analysis applications where efficient analyte mixing is essential.

ACKNOWLEDGMENT

This research is funded by Academy of Cryptography Techniques under grant number 08.DT22.C15.

REFERENCES

[1] K. Tsougeni *et al.*, "Plasma nanotextured polymeric lab-on-a-chip for highly efficient bacteria capture and lysis," *Lab Chip*, vol. 16, no. 1, pp. 120–131, 2016, doi: 10.1039/C5LC01217A.

[2] R. H. Phillips *et al.*, "Flow control using audio tones in resonant microfluidic networks: towards cell-phone controlled lab-on-a-chip devices," *Lab Chip*, vol. 16, no. 17, pp. 3260–3267, 2016, doi: 10.1039/C6LC00738D.

[3] X. Chen, C. Liu, Z. Xu, Y. Pan, J. Liu, and L. Du, "An effective PDMS microfluidic chip for chemiluminescence detection of cobalt (II) in water," *Microsyst. Technol.*, vol. 19, no. 1, pp. 99–103, Jan. 2013, doi: 10.1007/s00542-012-1551-8.

[4] E. O. Adekanmbi and S. K. Srivastava, "Dielectrophoretic applications for disease diagnostics using lab-on-a-chip platforms," *Lab Chip*, vol. 16, no. 12, pp. 2148–2167, 2016, doi: 10.1039/C6LC00355A.

[5] F. Yang, W. Zhao, and G. Wang, "Electrokinetic mixing of two fluids with equivalent conductivity," *Chinese J. Chem. Eng.*, vol. 42, pp. 256–260, Feb. 2022, doi: 10.1016/j.cjche.2021.03.032.

[6] J. . Rife, M. . Bell, J. . Horwitz, M. . Kabler, R. C. . Auyeung, and W. . Kim, "Miniature valveless ultrasonic pumps and mixers," *Sensors Actuators A Phys.*, vol. 86, no. 1–2, pp. 135–140, Oct. 2000, doi: 10.1016/S0924-4247(00)00433-7.

[7] S. O. Catarino, L. R. Silva, P. M. Mendes, J. M. Miranda, S. Lanceros-Mendez, and G. Minas, "Piezoelectric actuators for acoustic mixing in microfluidic devices—Numerical prediction and experimental validation of heat and mass transport," *Sensors Actuators B Chem.*, vol. 205, pp. 206–214, Dec. 2014, doi: 10.1016/j.snb.2014.08.030.

[8] C. Cavaniol, W. Cesar, S. Descroix, and J.-L. Viovy, "Flowmetering for microfluidics," *Lab Chip*, vol. 22, no. 19, pp. 3603–3617, 2022, doi: 10.1039/D2LC00188H.

[9] S. Rashidi, H. Bafekr, M. S. Valipour, and J. A. Esfahani, "A review on the application, simulation, and experiment of the electrokinetic mixers," *Chem. Eng. Process. - Process Intensif.*, vol. 126, pp. 108–122, Apr. 2018, doi: 10.1016/j.cep.2018.02.021.

[10] Y. Daghighi and D. Li, "Numerical study of a novel induced-charge electrokinetic micro-mixer," *Anal. Chim. Acta*, vol. 763, pp. 28–37, Feb. 2013, doi: 10.1016/j.aca.2012.12.010.

[11] K. Karthikeyan, L. Sujatha, and N. M. Sudharsan, "Numerical Modeling and Parametric Optimization of Micromixer for Low Diffusivity Fluids," *Int. J. Chem. React. Eng.*, vol. 16, no. 3, Mar. 2018, doi: 10.1515/ijcre-2016-0231.

[12] *Inst. Electr. Electron. Eng. Natl. Inst. Res. Dev. Microtechnologies (Romania), CAS 2012 Proc. 2012 Int. Semicond. Conf. 35th Ed. Oct. 15-17, 2012, Sinaia, Rom.*

[13] "Diffusion Equation," *https://www.comsol.com/multiphysics/diffusion-equation*. .

[14] "Navier-Stokes Equations," *https://www.comsol.com/multiphysics/navier-stokes-equations*. .

[15] A. P. P. ohn Evans, Dorian Liepmann, "PLANAR LAMINAR MIXER," *semanticscholar.org/paper/PLANAR-LAMINAR-MIXER-Evans-Liepmann/508af062de2926f943fbe1145aec2713bd6f4403*. .

THIẾT KẾ VÀ ĐÁNH GIÁ CẤU TRÚC TRỘN CHỮ T THỤ ĐỘNG VỚI CÁC TƯỜNG CẢN GẮN ĐUÔI

Nguyễn Văn Phú[1], Bùi Vân Anh[1], Phạm Văn Thành[1], Lưu Mạnh Quỳnh[2], Nguyễn Hoàng Nam[3], Nguyễn Chung Tiến[4], Nguyễn Thị Thanh Vân [4*]

[1] Khoa Vật lý, Trường Đại học Khoa học Tự nhiên, ĐHGQ Hà Nội

[2]Trung tâm Khoa học Vật liệu, Trường Đại học Khoa học Tự nhiên, ĐHGQ Hà Nội

[3] Trung tâm Nano và Năng lượng, Trường Đại học Khoa học Tự nhiên, ĐHGQ Hà Nội

[4]Học viện Kỹ thuật Mật mã

*Email: nguyenthithanhvancms@gmail.com

TÓM TẮT

Trong bài báo này, mô hình bộ vi trộn dạng chữ T có cấu trúc tường cản được thiết kế và khảo sát bằng phương pháp tính toán số nhằm khảo sát nâng cao hiệu quả trộn. Mô hình trộn thụ động của cấu trúc tường cản thông thường được đề xuất bổ sung thêm phần đuôi tường đã được nghiên cứu và so sánh với các bộ vi trộn chữ T thông thường khác. Hiệu suất trộn của các cấu trúc được đánh giá thông qua việc

tính toán sử dụng phần mềm mô phỏng. Bộ trộn chữ T vi mô với các tường cản gắn đuôi (μTTAO) đề xuất cho thấy hiệu quả trộn cao hơn và đạt mức 87,2%. Ngoài ra, khoảng giá trị nồng độ theo mặt cắt lối ra cũng được thu hẹp, hiệu suất trộn tăng khoảng 1,41 so với bộ trộn chữ T thông thường. Sự kết hợp của các tường cản giúp cải thiện đáng kể hiệu quả trộn do sự nhiễu loạn của dòng chảy. Bên cạnh đó, việc kết hợp của nhiều chướng ngại vật trong cấu trúc vi lỏng giúp nâng cao hiệu suất của bộ trộn và giảm thời gian trộn. Ngoài ra, ảnh hưởng của độ dài và số lượng tường cản trong vi kênh đến hiệu suất trộn cũng đã được triển khai tính toán và phân tích, đánh giá trong nghiên cứu này. Kết quả cho thấy việc tăng số lượng hoặc độ dài của tường cản trong vi kênh sẽ cải thiện và tối ưu hiệu quả trộn. Nghiên cứu cũng chỉ ra rằng cấu trúc μTTAO đề xuất là một cấu trúc tiềm năng và có thể trở thành nền tảng để tối ưu hóa hiệu suất trộn của bộ vi trộn dạng chữ T, điều này có ý nghĩa rất quan trọng cho việc phát triển các bộ vi trộn có hiệu suất trộn cao và chi phí thấp trong tương lai.

Từ khoá: Grooves, mô hình trộn, trộn thụ động, dạng chữ T.

Nguyễn Văn Phú sinh ngày 01/07/2000 tại Thái Nguyên. Ông tốt nghiệp cử nhân ngành Vật lý năm 2022 và học viên cao học chuyên ngành Vật lý Vô tuyến và Điện tử tại Trường Đại học Khoa học Tự nhiên - ĐHQGHN. Hiện nay, ông công tác tại Khoa Vật lý, Trường Đại học Khoa học Tự nhiên, Đại học Quốc gia Hà Nội.

Lĩnh vực nghiên cứu: Hệ thống vi cơ điện tử (MEMS), Điện tử y sinh, Vật lý Vô tuyến và Điện tử.

Bùi Vân Anh sinh ngày 30/03/2002 tại Sơn La. Bà hiện đang học cử nhân ngành Vật lý tại trường Đại học Khoa học Tự nhiên, Đại học Quốc gia Hà Nội.

Lĩnh vực nghiên cứu: Hệ thống vi cơ điện tử (MEMS), Điện tử y sinh, Vật lý Vô tuyến và Điện tử.

Phạm Văn Thành sinh ngày 16/07/1984 tại Hải Dương. Ông tốt nghiệp cử nhân ngành Vật lý năm 2006 và thạc sĩ chuyên ngành Vật lý Vô tuyến và Điện tử tại Trường Đại học Khoa học Tự nhiên - ĐHQGHN vào năm 2009. Ông nhận học vị tiến sĩ năm 2012 tại Viện Khoa học và Công nghệ Tiên tiến Nhật Bản. Hiện nay, ông công tác tại khoa Vật lý, Trường Đại học Khoa học Tự nhiên, Đại học Quốc gia Hà Nội.

Lĩnh vực nghiên cứu: Vật lý Vô tuyến và Điện tử.

Lưu Mạnh Quỳnh sinh ngày 10/12/1980. Ông tốt nghiệp ThS. Vật lý Sinh học năm 2005 tại Đại học Eotvos Lorand, Budapest, Hungary. Ông nhận học vị tiến sĩ năm 2020, ngành Vật lý chất rắn. Hiện nay, ông công tác tại Trung tâm Khoa học Vật liệu, khoa Vật lý, Trường Đại học Khoa học Tự nhiên, Đại học Quốc gia Hà Nội.

Lĩnh vực nghiên cứu: Vật liệu nano ứng dụng, Vật lý sinh học

Nguyễn Hoàng Nam sinh ngày 5/8/1979 tại Hà Nội. Ông tốt nghiệp cử nhân và thạc sỹ ngành Vật lý năm 2004 tại trường Đại học Eotvos Lorand, Budapest, Hungary. Ông nhận học vị tiến sĩ ngành Vật lý năm 2008 tại Đại học Osaka, Nhật Bản và được phong học hàm phó giáo sư năm 2017. Hiện nay, ông công tác tại khoa Vật lý và Trung tâm Nano và Năng lượng, Trường Đại học Khoa học Tự nhiên, Đại học Quốc gia Hà Nội.

Lĩnh vực nghiên cứu: Vật liệu nano và cảm biến, thiết bị điện tử y sinh.

Nguyễn Chung Tiến sinh ngày 3/11/1974 tại Hà Nội. Ông tốt nghiệp trình độ Đại học chuyên ngành Kỹ thuật mật mã năm 1996 và thạc sĩ Công nghệ thông tin tại Viện Tin Học Pháp ngữ vào năm 2001. Ông nhận học vị tiến sĩ Công nghệ thông tin năm 2008. Hiện nay, ông công tác tại Học viện Kỹ thuật mật mã về lĩnh vực bảo mật và an toàn thông tin.

Lĩnh vực nghiên cứu: An toàn thông tin, vật lý ứng dụng trong an toàn thông tin.

Nguyễn Thị Thanh Vân sinh ngày 04/12/1982 tại Hà Nội. Bà tốt nghiệp cử nhân ngành Vật lý năm 2004 và thạc sĩ chuyên ngành Vật lý Chất rắn tại Trường Đại học Khoa học Tự nhiên - Đại học Quốc Gia Hà Nội năm 2006. Bà nhận học vị tiến sĩ năm 2013 tại Trường Đại học Khoa học Tự nhiên – Đại học Quốc Gia Hà Nội. Hiện nay, bà công tác tại Học viện Kỹ thuật Mật mã - Ban Cơ yếu Chính phủ.

Lĩnh vực nghiên cứu: Vật liệu, ứng dụng vật liệu trong mật mã.